FENS-1 and DFCP1 are FYVE domain-containing proteins with distinct functions in the endosomal and Golgi compartments

S. H. Ridley[1], N. Ktistakis[1], K. Davidson[1], K. E. Anderson[1], M. Manifava[1], C. D. Ellson[1], P. Lipp[2], M. Bootman[2], J. Coadwell[1], A. Nazarian[3], H. Erdjument-Bromage[3], P. Tempst[3], M. A. Cooper[4], J. W. J. F. Thuring[4], Z.-Y. Lim[4], A. B. Holmes[4], L. R. Stephens[1] and P. T. Hawkins[1,*]

[1]Inositide Laboratory, The Babraham Institute, Babraham, Cambridge CB2 4AT, UK
[2]Laboratory of Molecular Signalling, The Babraham Institute, Babraham, Cambridge CB2 4AT, UK
[3]Memorial Sloan-Kettering Cancer Center, New York, NY10021, USA
[4]Department of Chemistry, Cambridge University, Lensfield Road, Cambridge CB2 1EW, UK
*Author for correspondence (e-mail: phillip.hawkins@bbsrc.ac.uk)

Accepted 26 July 2001
Journal of Cell Science 114, 3991-4000 (2001) © The Company of Biologists Ltd

SUMMARY

FENS-1 and DFCP1 are recently discovered proteins containing one or two FYVE-domains respectively. We show that the FYVE domains in these proteins can bind PtdIns3P in vitro with high specificity over other phosphoinositides. Exogenously expressed FENS-1 localises to early endosomes: this localisation requires an intact FYVE domain and is sensitive to wortmannin inhibition. The isolated FYVE domain of FENS-1 also localises to endosomes. These results are consistent with current models of FYVE-domain function in this cellular compartment. By contrast, exogenously expressed DFCP1 displays a predominantly Golgi, endoplasmic reticulum (ER) and vesicular distribution with little or no overlap with FENS-1 or other endosomal markers. Overexpression of DFCP1 was found to cause dispersal of the Golgi compartment defined by giantin and gpp130-staining. Disruption of the FYVE domains of DFCP1 causes a shift to more condensed and compact Golgi structures and overexpression of this mutant was found to confer significant protection to the Golgi against brefeldin-induced dispersal. These properties of DFCP1 are surprising, and suggest FYVE domain-localisation and function may not be exclusively endosomal.

Movies available on-line

Key words: FYVE domain, PtdIns3P, Endosomes, Golgi, Vesicle trafficking

INTRODUCTION

Phosphoinositides are membrane phospholipids that are known to regulate the membrane location and activities of specific families of proteins that possess one or more lipid-binding homology domains. One clear example of this principle is in intracellular signalling, where certain PH domains drive the recruitment of key signalling intermediates to PtdIns(3,4,5)P_3 and/or PtdIns(3,4)P_2 generated at the plasma membrane by receptor activation of class I PI3 kinases (Lemmon and Ferguson, 2000). Another clear example is in intracellular trafficking, where FYVE domain binding to PtdIns3P, generated by class III PI3-kinases, is thought to play a major role in the endosomal localisation and function of proteins in this compartment (Gaullier et al., 1998; Burd and Emr, 1998).

Using a targeted proteomics approach with phosphoinositide-linked affinity matrices we recently identified two novel FYVE domain-containing proteins, originally catalogued as SR1 and SR3 (Krugmann et al., unpublished). SR1 is renamed here FENS-1 (FYVE domain containing protein localised to endosomes)-1; SR3 is identical to DFCP1, which has been recently isolated in parallel from a human bone marrow cDNA library (Derubeis et al., 2000). FENS-1 contains a single FYVE domain and multiple WD-40 repeats. DFCP1 uniquely has tandem FYVE domains at its C terminus, together with another putative C_2H_2 type zinc finger at its N terminus and also a possible nucleotide binding P-loop (Fig. 1). We have attempted to define the phosphoinositide binding specificities of FENS-1 and DFCP1, and the role these play in the localisation and function of the two proteins in the cell.

MATERIALS AND METHODS

The synthesis of PtdIns3P and PtdIns(3,4)P_2-linked Sepharose beads is described elsewhere (Painter et al., 2001). All phosphoinositides used in these experiments were the dipalmitoyl esters (Painter et al., 1999). Stocks of the lipids (4-10 mM) were prepared by bath sonication of dried powders into H_2O for PtdIns(3,4,5)P_3, PtdIns(3,4)P_2, PtdIns(4,5)P_2 and PtdIns(3,5)P_2 and into DMSO for PtdIns4P, PtdIns5P and PtdIns3P: these stocks were stored briefly at –20°C and diluted (to ≤500 μM) into assay buffers containing micellar NP-40. The human cDNAs encoding FENS-1 and DFCP1 were isolated as described elsewhere (Krugmann et al., unpublished) (EMBL Accession Numbers AJ310568 and AJ310569) and subcloned into pCMV3myc (Stephens et al., 1997) and pEGFPC2 (Clontech) vectors using standard procedures. Site-

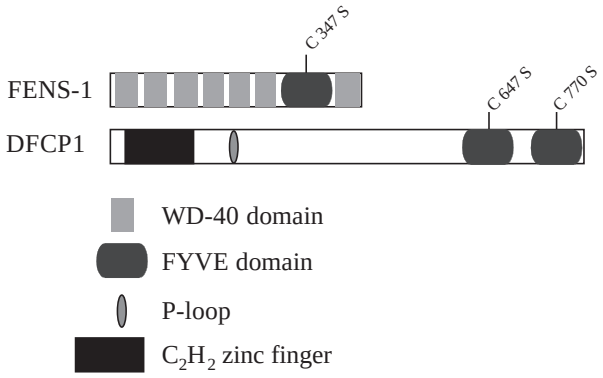

Fig. 1. Schematic domain profile for FENS-1 (originally catalogued as SR1; Accession Number, AJ310568) and DFCP1 (originally catalogued as SR3; Accession Number, AJ310569), also showing point mutations generated.

directed mutagenesis was performed by PCR using Stratagene 'Quick change protocol' and all constructs were verified by DNA sequencing. Mouse anti-Myc monoclonal 9E10 was prepared at the Babraham Institute. Rabbit anti-Myc polyclonal was from Santa Cruz. Mouse anti-EE ascites was from BABCO. Rabbit anti-GFP polyclonal was from Clontech. Rabbit anti-giantin was a gift from Dr Sean Munro (MRC Laboratory of Molecular Biology, Cambridge, UK). Rabbit anti-gpp130 was a gift from Dr Hans-Peter Hauri (Biozentrum of the University of Basel, Switzerland). Rabbit anti-EEA1 was from Transduction Laboratories. Mouse monoclonal antibodies against KDEL receptor and β-COP were from Sigma. An expression vector for GFP-elastase was a gift from Dr Etienne Joly (CNRS, Toulouse, France).

Preparation of recombinant EE-FENS-1 and EE-DFCP1

The pAcoGEE transfer vector (Stephens et al., 1997) was used for baculovirus-driven expression of N-terminal EE-tag FENS-1 and DFCP1 in SF9 cells. SF9 cells (European Tissue Culture Collection) were grown in suspension culture (0.5-2.0×10^6 cells ml^{-1}) for up to 10 weeks in TNM-FH medium supplemented with 11% foetal bovine serum (heat-inactivated) and antibiotics (penicillin/streptomycin). Transfer vectors were co-transfected with linearised baculovirus DNA (Baculo-gold, Pharminogen) into SF9 cells using cationic liposomes (Insectin, Pharminogen) as recommended. Recombinant viruses were plaque-purified and amplified via three cycles of infection to yield high titre virus stocks (>10^8 infection particles ml^{-1}). Protein production was optimised for each construct. Typically, protein was purified from the equivalent of 2-4 l of culture, infected at 10^6 cells ml^{-1} with 0.5-1.0% (v/v) of high titre viral stock, and cultured for 1.8-2.5 days. The cells were harvested, washed once in TNM-FH and snap-frozen in liquid N_2. The pellets were thawed and sonicated into lysis buffer (1% (w/v) Triton X-100; 0.15 M NaCl; 40 mM Hepes-NaOH, pH 7.4 at 4°C; 1 mM DTT, 0.1 mM PMSF, 10 μg ml^{-1} of antipain, pepstatin A, aproptinin and leupeptin). Proteins were purified via their EE-tags as follows. Homogenates were centrifuged (100,000 ***g*** for 60 minutes) and mixed with EE-beads (anti-EE monoclonal antibody, dimethyl pimelimidate-crosslinked to Protein G-Sepharose; capacity ~2 mg of a 50 kDa target protein ml^{-1} beads). Immunoprecipitation (90 minutes, end-on-end at 4°C) was followed by washing (four times with 0.1% w/v Triton X-100; 0.3 M NaCl; 20 mM Hepes/NaOH, pH 7.4, 1 mM DTT; and three times with phosphate-buffered saline (PBS) containing 1 mM DTT and either 10% or 20% (v/v) ethylene glycol for EE-DFCP1 or EE-FENS-1, respectively). Proteins were eluted with 100 μg ml^{-1} of peptide EEYMPME (N-terminal acetylated) in the relevant final wash buffer. One volume of protein-loaded beads was incubated three to four times for 20 minutes on ice (with occasional mixing) with 1 volume of elution buffer, and centrifuged. The pooled supernatants were concentrated (Centriplus concentrators; Amicon) to ≤2.5 ml and passed through a PD-10 column (Pharmacia) (in elution buffer without peptide). Protein-containing fractions were further concentrated, snap-frozen and stored. Protein concentrations were determined by a combination of SDS-PAGE followed by Coomasie staining and Bradford protein assay (BioRad), with BSA standard (correcting for the fact that BSA gives a colour yield 1.29-fold greater than for an average range of proteins).

Preparation of recombinant FYVE domain of FENS-1

The isolated FYVE domain [274-358]FENS-1 was subcloned into the GST N-terminal fusion expression vector pGEX4T1 (AmershamPharmaciaBiotech) and transformed into *E. coli* stain BL21DE3pLysS (Stratagene). Transformants were grown to logarithmic growth phase at 30°C before induction with 1 mM IPTG for 4 hours. Cells were lysed by freeze-thaw followed by probe sonication in PBS with 1 mM DTT. Triton X-100 was added to 1% (v/v) and the lysate was left on ice for 20 minutes before centrifugation (100,000 ***g***, 60 minutes, 4°C). The supernatant was mixed with glutathione sepharose beads (AmershamPharmaciaBiotech) for 1 hour at 4°C. The beads were washed seven times with PBS, 1% (v/v) Triton X-100, 1 mM DTT and 0.1 M NaCl and 5 times with PBS plus DTT alone. FENS-1(273-358) was removed from the beads by thrombin cleavage (20 U/ml, 16 hours, 4°C) yielding a 0.8 mg ml^{-1} stock in PBS, 1 mM DTT.

Transient transfection of mammalian cells

COS-7 cells were maintained in DMEM supplemented with 10% (v/v) FCS (Gibco BRL) at 37°C in a humidified atmosphere of 5% CO_2. Porcine aortic endothelial cells (PAE) were maintained in Ham's F12 medium with 10% FCS. For the bulk of the immunohistochemical experiments with COS-7 cells, cells were seeded onto glass coverslips in six well (35 mm diameter) plates 24 hours before transfection with DEAE dextran. Cells were washed twice (over 20 minutes, at 37°C) with serum-free DMEM plus 10 mM Hepes-NaOH, pH 7.2 (wash medium). Plasmid DNA (1-3 μg/well) was then mixed with DEAE-dextran (250 μg/ml wash medium) and added to the cells (800 μl/well), which were left for 2 hours at 37°C, with swirling every 30 minutes. The DNA mixture was then replaced with 3 ml DMEM plus 10% FCS containing 100 μM chloroquinne, and the cells were left for a further 4.5 hours at 37°C. The cells were then washed twice and harvested 36 hours later. For all the experiments designed to produced recombinant protein in COS-7 cell lysates for 'bead-displacement assays' and for some of the immunohistochemical experiments with COS-7 cells, and all of the immunohistochemical experiments with PAE cells, cells were transfected by electroporation as described elsewhere (Anderson et al., 1998).

Immunocytochemistry

Cells were washed in PBS and were fixed either by immersion for 5 minutes in methanol (pre-cooled to –20°C) or incubation with 3.75% (w/v) paraformaldehyde in 200 mM Hepes-NaOH, pH 7.2 for 20 minutes at room temperature. In the latter case, cells were then washed three times over 15 minutes with serum-free DMEM post fixation and permeabilised with 0.1% (v/v) Triton X-100 in PBS for 10 minutes. The cells were then washed three times with PBS alone. For immunostaining, cells were first incubated with PBS/1% (w/v) BSA for 30 minutes. Primary antibodies were diluted in PBS/BSA and incubated with the cells for 30 minutes at room temperature. Fluorophore-conjugated secondary antisera (Jackson Immunoresearch) were diluted in PBS/BSA for 30 minutes at room temperature. Cells were washed three times for 5 minutes with PBS/BSA between additions. Coverslips were mounted onto glass slides with Aqua Polymount (Polyscience) and were viewed using either a Zeiss Axiophot fluorescence microscope with a digital camera (either Spot Colour, Diagnostic Instruments or Orca, Hamamatsu

Phototronics). Merging of digital images was performed using Adobe Photoshop. For live cell imaging, a heated-stage Olympus IX70 microscope was used, interfaced with an 'Ultraview' confocal system (Perkin-Elmer Life Sciences).

Transport of influenza virus hemagglutinin

COS-7 cells were transfected with plasmid pCB6 encoding the hemagglutinin (HA) protein (Brewer, 1994), plus plasmids encoding various forms of FENS-1, DFCP1 or Arf1 (kindly provided by Dr J. Donaldson). Forty hours after transfection, the cells were lysed and the HA protein was immunoprecipitated using monoclonal antibody FC-125 (kindly provided by Dr T. Braciale) as described previously (Ktistakis et al., 1995). Following SDS-PAGE and electroblotting, the immunoprecipitated HA was visualised with polyclonal anti-HA antibodies (kindly provided by Dr M. Roth).

Bead-displacement assays

For analysis of GFP or Myc-tagged proteins expressed in COS-7 cell lysates approx. 1×10^7 cells were transfected by electroporation with 20 μg DNA and allowed to recover for 36-48 hours in DMEM 10% FCS in two 15 cm petri dishes. Cells were washed in ice-cold PBS and each plate lysed on ice into 5 ml of 1% (v/v) NP-40, 20 mM Hepes-NaOH, pH 7.4 at 5°C, 0.125 M NaCl, 5 mM EDTA, 5 mM EGTA, 5 mM β-glycerophosphate, 10 mM NaF, 1 mM orthovanadate (in some experiments EDTA and EGTA were replaced with 1 mM $MgCl_2$). Lysates were scraped, combined and centrifuged at approx. 190,000 ***g*** for 20 minutes at 4°C. Aliquots of supernatant were then used directly or snap-frozen in liquid N_2 and stored at –80°C for later use.

These aliquots were diluted between 1.1- to 1.5-fold for GFP-FENS constructs and between three- and fourfold for DFCP1 constructs with lysis buffer before mixing with the indicated concentrations of phosphoinositides (usually diluted from 5-10× stocks prepared in lysis buffer) in a total volume of 1 ml. The samples were mixed and incubated on ice for 10-15 minutes and then transferred onto 10-20 μl packed phosphoinositide beads (prequilibrated in wash buffer – see below) and mixed end/end at 4°C for approx. 45 minutes Beads were centrifuged and washed four times in the lysis buffer described above (except 1% NP-40 was replaced with 0.1% NP-40; the total wash time for batches of samples was always ≤15 minutes). Proteins were eluted from the beads with 30 μl of SDS sample buffer, separated by SDS PAGE, transferred to Immobilon P (Millipore) and detected by the appropriate Western blotting procedure (anti-EE, anti-Myc or anti-GFP). For bead-displacement assays using recombinant EE-tagged FENS-1 and DFCP1 the assay followed the format described above except that the proteins (0.2 μM) were mixed with phosphoinositides and the beads were washed in PBS, 0.1% NP-40, with or without 1 mM $MgCl_2$.

Surface plasmon resonance measurements of recombinant EE-FENS-1 and DFCP1 binding to lipid surfaces

Recombinant proteins were analysed for their ability to bind to low molar percentage phosphoinositides in a lipid background by surface plasmon resonance using vesicle capture onto a Biacore L1 sensor chip or self assembled lipid monolayer onto a Biacore HPA sensor chip. The phosphoinositides PtdIns(3,4)P_2, PtdIns(3,5)P_2, PtdIns(4,5)P_2 and PtdIns(3,4,5)P_3 were manually injected onto the self assembled monolayer of PC/PE/PS (1:1:1) at 6% (w/w) of the total lipid assembled. The phosphoinositides PtdIns3P and PtdIns5P were incorporated into vesicles at 6% (w/w) before assembly on the sensor chip surface, either in PC alone or in a 1:1:1 mixture of PC/PE/PS. Binding was carried out at a flow rate of 10 μl min^{-1} with 6 minutes association and 6 minutes dissociation in PBS with 1 mM $MgCl_2$.

Online supplemental material

Videos describing live image recording of GFP-FENS-1 (Movie A), GFP-DFCP1 (Movie B) and GFP-iFYVE FENS-1 (Movie C) (still images from these videos are presented in Figs 4 and 6) can be viewed at jcs.biologists.org/supplemental.

RESULTS

FENS-1 and DFCP1 bind PtdIns3P

FENS-1 and DFCP1 were originally isolated by us as part of a targeted proteomics strategy to isolate novel phosphoinositide-binding proteins. FENS-1 was originally isolated on PtdIns3P beads from both pig platelet and sheep liver cytosol and on PtdIns(3,4)P_2 beads from pig platelet cytosol: DFCP1 was originally isolated on PtdIns(3,4)P_2 beads from sheep brain cytosol (Krugmann et al., unpublished). The cDNAs encoding the human forms of FENS-1 and DFCP1 were cloned (Fig. 1) and used to express variously tagged recombinant proteins in both mammalian cells and baculovirus-infected Sf9 cells.

We began to define a phosphoinositide-binding specificity for these proteins by investigating the ability of different individual phosphoinositides to compete for binding to these proteins with the phosphoinositide moiety covalently attached to the beads. We have found that in the presence of micellar NP-40 and physiological salt concentrations, these assays can give very clear and informative data about the head group specificity of phosphoinositide-binding proteins (Krugmann et al., unpublished). We conducted a range of assays in this format using newly synthesised PtdIns3P beads, newly synthesised PtdIns(3,4)P_2 beads and PtdIns(3,4)P_2 beads previously exposed to tissue extracts and probably containing a mixture of PtdIns3P, PtdIns4P and PtdIns(3,4)P_2, owing to phosphatase action (we suspect these beads have the advantage of presenting PtdIns3P in a more generally 'protein-repellent' surface – data not shown). The results suggest both FENS-1 and DFCP1 have a clear preference for binding PtdIns3P relative to all other phosphoinositides known to be present in mammalian cells (Fig. 2 and data not shown). This is a property of both N-terminal Myc or N-terminal GFP-tagged FENS-1 and N-terminal Myc-tagged DFCP1 expressed and assayed in COS-7 cell lysates in the presence of excess EDTA/EGTA or in the absence of EDTA/EGTA and 1 mM added $MgCl_2$ (Fig. 2; and data not shown). N-terminal EE tagged FENS-1 and DFCP1 purified from baculovirus-infected SF9 cells also display a binding preference for PtdIns3P when assayed in the presence or absence of 1 mM $MgCl_2$ (data not shown).

We created single point mutants in the FYVE finger domains of FENS-1 (C347S) and DFCP1 (C647S and C770S) by analogy to previously defined critical cysteine residues required for PtdIns3P binding to FYVE domains in other proteins (Gaullier et al., 1998). These cysteine residues are required for Zn binding, and it is likely that their mutation will significantly affect the three-dimensional structure of the FYVE domains. However, the comparable expression levels of the mutants and the wild-type proteins suggest that gross misfolding is unlikely to occur. Negligible binding of [C347S] FENS-1 and [C647S/C770S]DFCP1 to the phosphoinositide beads was observed (Fig. 2), confirming the importance of the FYVE-domain in mediating the binding of both of these proteins to these beads in vitro and the critical function of these particular residues in this process. Use of the individual mutations within each of the two FYVE domains of DFCP1 suggested both domains were required for maximal binding to the beads but

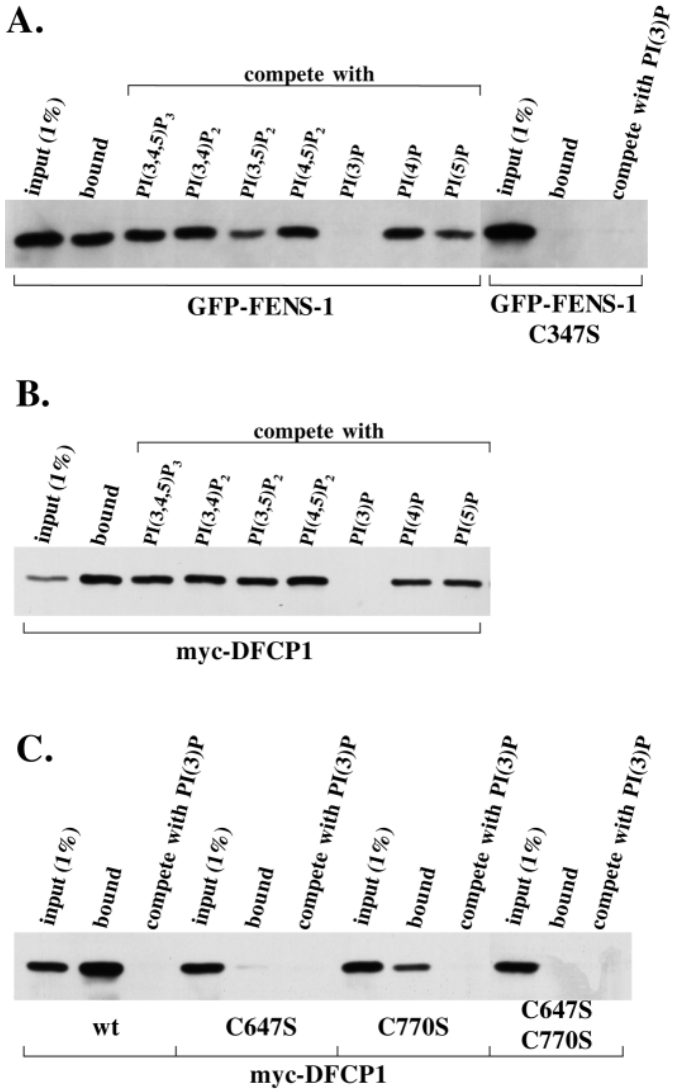

Fig. 2. Analysis of phosphoinositide binding specificities of GFP-FENS-1 (A) and Myc-DFCP1 (B,C) constructs expressed in COS-7 cell lysates using lipid competition for binding to phosphoinositide-derivatised beads. The indicated GFP-tagged FENS-1 constructs or Myc-tagged DFCP1 constructs were expressed in COS-7 cells and lysates prepared as described in the Materials and Methods. Aliquots of these lysates were mixed with the indicated phosphoinositides (5 μM and 10 μM for FENS-1 and DFCP1, respectively) in a total volume of 1 ml for 10 minutes on ice, then transferred onto 15 μl packed PtdIns(3,4)P_2-derivatised beads and mixed end to end at 4°C for 45 minutes. Beads were washed briefly four times and the recovery of the relevant proteins was assessed by SDS PAGE and the appropriate Western-blotting procedure (see Materials and Methods). 1% aliquots of the various lysates were taken before mixing with the beads to assess relative expression levels and recovery on the beads of each construct.

that the C647S mutation had significantly the greater effect (Fig. 2C), suggesting these assays predominantly measure the lipid-binding characteristics of the more N-terminal of the two FYVE domains in this protein.

We investigated the binding of purified, recombinant EE-FENS-1 to lipid monolayers self-assembled on alkane-coated gold surfaces (HPA chips) (Cooper et al., 1998) or to small unilamellar liposomes trapped on alkane-derivatised, dextran coated gold surfaces (L1 chips) (Cooper et al., 2000) using a surface plasmon resonance (SPR) biosensor. EE-FENS-1 had very low binding to PE/PS/PC monolayers or to PC liposomes in the presence of PBS, 1 mM $MgCl_2$ (Fig. 3A,B and data not shown). The binding of EE-FENS-1 to these monolayers was dramatically enhanced by the inclusion of low mole % PtdIns3P but not other phosphoinositide species (Fig. 3B). A simple 1:1 binding analysis (Langmuir) of the association/dissociation kinetics of EE-FENS-1 binding to PC liposomes containing 1 mole% PtdIns3P gives an approximate K_D of 48 nM (χ^2=0.7). This suggests that the presence of PtdIns3P in a membrane surface is a likely significant driving force for a shift in equilibrium position for FENS-1 between soluble and membrane-bound locations. Further, the ability of a purified, isolated FYVE-domain of FENS-1 to exhibit similar binding characteristics suggests this property is dictated by the FYVE-domains itself (Fig. 3C).

We also investigated the binding of recombinant EE-DFCP1 to lipid surfaces using similar surface plasmon resonance assays to those described above for EE-FENS-1. We observed very high, variable binding of EE-DFCP1 to the background lipid surfaces used (which included 1:1:1 mixtures of PE/PC/PS or individual surfaces of PI, PC, or PS) making it difficult to assess the impact of including low mole % phosphoinositides – an example of the data obtained is given in Fig. 3D. Recombinant EE-DFCP1 clearly has a much higher affinity for the background lipid surfaces used than EE-FENS-1, and the potential impact of PtdIns3P on the membrane localisation of this protein is far less clear.

Exogenously-expressed FENS-1 and DFCP1 exhibit different subcellular distributions

We wished to relate the lipid binding properties of FENS-1 and DFCP1 to their subcellular localisations and possible functions. COS-7 cells were transiently transfected with plasmids expressing N-terminal fusions of either Myc- or GFP-tagged FENS-1 or DFCP1 and the localisations of exogenously expressed proteins were visualised in methanol- or paraformaldehyde-fixed cells by indirect immunofluorescence, or in live cells by direct, real-time video-imaging of GFP fluorescence. For each protein, essentially similar cellular localisations were seen between either tag and between fixed cells and live imaging except that some consistent quantitative differences were observed between GFP-DFCP1 and Myc-DFCP1. FENS-1 localised to clear, dynamic, punctate structures of differing size and morphology (either small and vesicular or larger and vacuolar) and in the most highly expressing cells, it showed variable accumulation in the cytosol and nuclear compartments (Fig. 4). DFCP1 had a complex distribution consisting of a fine reticular network, a strong perinuclear presence and a variable number of small, dynamic vesicular structures which did not overlap with co-expressed FENS-1 (Fig. 4): this distribution is consistent with images shown of exogenous DFCP1 expression in NIH3T3 cells (Derubeis et al., 2000).

Exogenously-expressed FENS-1 is found in early endosomes

The punctate structures containing FENS-1 were identified as early endosomes on the basis of strong colocalisation in fixed cells with endogenous EEA1 (Fig. 5). It appeared that

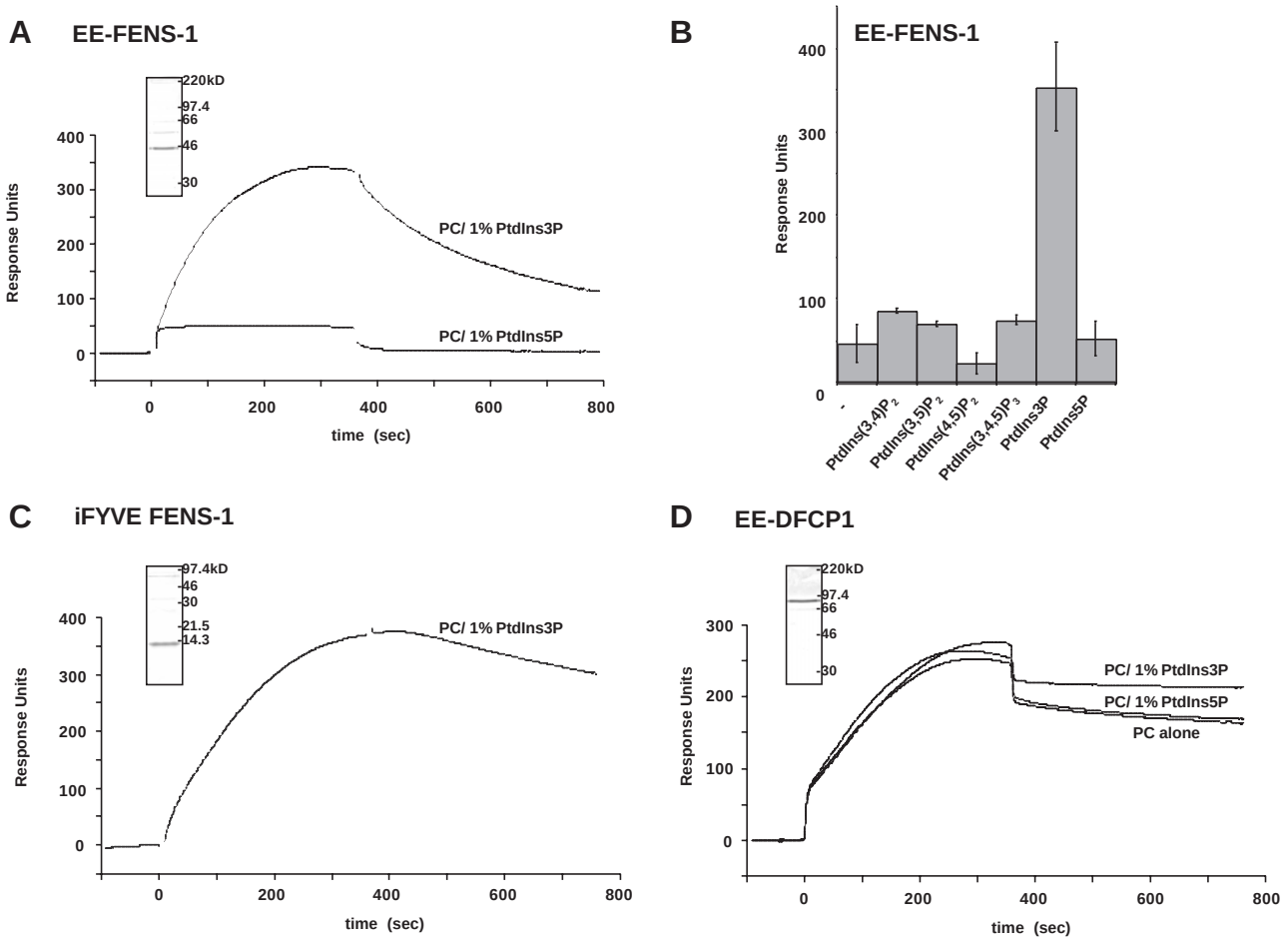

Fig. 3. Analysis of recombinant EE-FENS-1, iFYVE FENS-1 and EE-DFCP1 binding to lipid surfaces using BiaCore. (A) Sensorgrams describing the binding of EE-FENS-1 to PC liposomes containing 1 mole% PtdIns3P or 1 mole% PtdIns5P captured on an L1 sensor chip. Binding of EE-FENS-1 to PC alone was low (approx. 20 response units at equilibrium) and this sensorgram has been subtracted from the two shown to remove bulk refractive-index changes that are due to the ethylene-glycol-containing FENS-1 solution. 100 nM FENS-1 diluted into PBS, 1 mm $MgCl_2$ was injected at t=0 for 360 seconds (at 10 μl min^{-1}) and then the dissociation followed for a further 400 seconds. The inset shows a Coomassie-stained SDS PAGE gel of approx. 2 μg of recombinant EE-FENS. (B) Binding of EE-FENS-1 to PC monolayers alone or containing 6 mole% phosphoinositides, assembled on an HPA sensor chip. The values shown are the means±s.e.m. (n=2-4) for the binding of approx. 100 nM EE-FENS-1 at equilibrium. (C) Sensorgram describing the binding of iFYVE FENS-1 to a PE/PC/PS (1:1:1 mole ratios) monolayer containing 1 mole% PtdIns3P assembled on an HPA sensor chip. Binding of iFYVE FENS-1 to PE/PC/PS surfaces only was low (approx 26 response units at equilibrium) and this sensorgram has been subtracted from the one shown to remove bulk refractive index changes caused by the glycerol-containing iFYVE FENS-1 solution. 100 nM iFYVE FENS-1 diluted into PBS, 1 mM $MgCl_2$ was injected at t=0 for 360 seconds (at 10 μl min^{-1}) and then dissociation followed for a further 400 seconds. The inset shows a Coomasie-stained SDS PAGE gel of approx 2 μg thrombin-cleaved, recombinant iFYVE FENS-1. (D) Sensorgrams describing the binding of EE-DFCP1 to PC liposomes alone or containing 1 mole% PtdIns3P or PtdIns5P, captured on an L1 sensor chip. 50 nM EE-DFCP1 diluted into PBS, 1 mM $MgCl_2$ was injected at t=0 for 360 seconds (at 10 μl min^{-1}) then dissociation followed for a further 400 seconds. The instant refractive index changes at the point of injection and dissociation are caused by the bulk refractive index changes to and from the ethylene glycol containing EE-DFCP1 solution. The inset shows a Coomassie-stained SDS PAGE gel of approx 2 μg EE-DFCP1.

overexpression of FENS-1 caused the accumulation of EEA1 into fewer, more irregular-shaped vesicles that represent the vacuolar structures described above. This effect was seen in both PAE and COS-7 cells, although it was generally more marked in the latter, possibly because of increased exogenous expression of FENS-1 (data not shown).

The localisation of FENS-1 to early endosomes requires an intact FYVE domain and is inhibited by wortmannin

COS-7 cells expressing either GFP- or Myc-tagged FENS-1 were treated with the PI3-kinase inhibitor wortmannin and this resulted in a loss of punctate FENS-1 staining (Fig. 6 and data not shown): this effect can be viewed in real time in Movie A. By contrast, the endosomal localisation of EEA1 in untransfected cells was much less sensitive to wortmannin (data not shown).

The role of the FYVE domain in the localisation of FENS-1 was investigated using the FYVE domain mutant, GFP-[C347S]FENS-1 and the isolated FYVE domain itself, GFP-iFYVE FENS-1 (residues 274-358). The localisation of GFP-[C347S]FENS-1 was cytosolic with no punctate staining (Fig. 6, insert). The localisation of GFP-iFYVE FENS-1 was almost identical to the wild-type protein (Fig. 5) showing

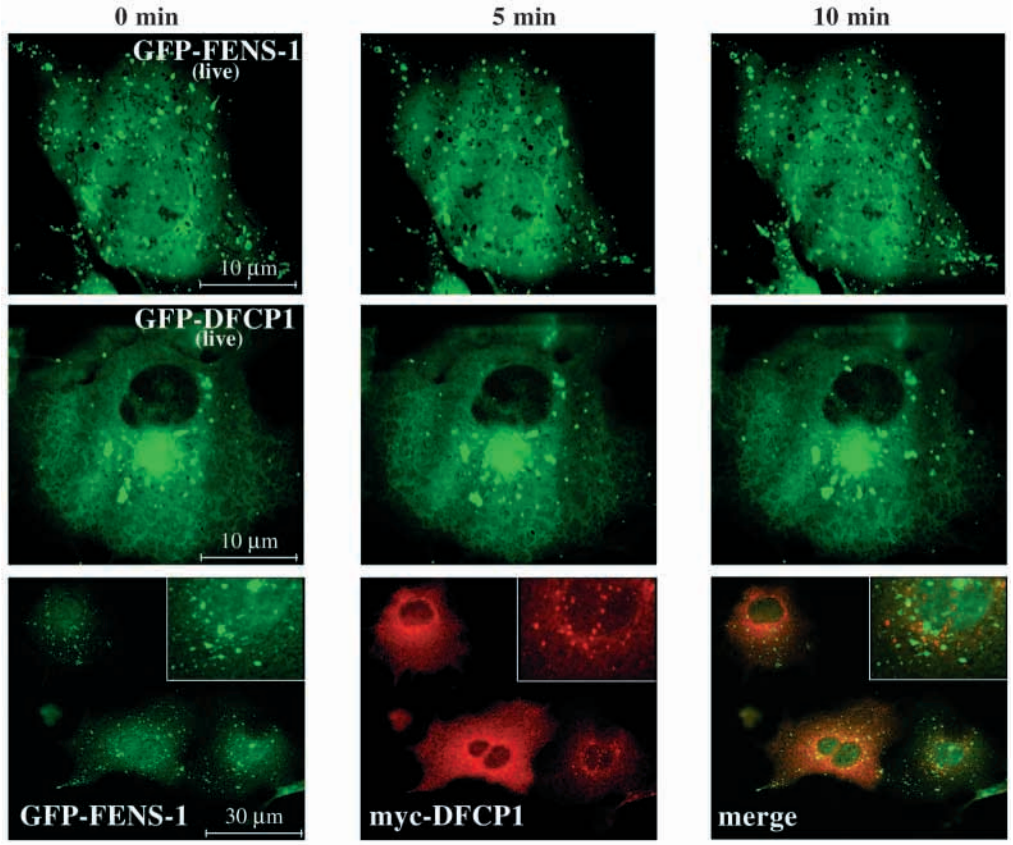

Fig. 4. Subcellular localisation of exogenously expressed FENS-1 and DFCP1. Top two panels: COS-7 cells were transfected with expression vectors encoding GFP-FENS-1 and GFP-DFCP1 and processed for live image recording of GFP-fluorescence as described in the Materials and Methods. The images shown represent stills taken from Movies A and B describing GFP-FENS-1 and GFP-DFCP1, respectively: the movies can be viewed at jcs.biologists.org/supplemental. Lower panel: COS-7 cells were co-transfected with expression vectors encoding GFP-FENS-1 and Myc-DFCP1. The cells were fixed with methanol and processed for direct (GFP) and indirect (Texas-Red, anti-Myc) fluorescence as described in the Materials and Methods.

strong co-distribution with co-expressed Myc-FENS-1 (data not shown) and endogenous EEA1 (Fig. 5). The distribution of EEA1 was affected by GFP-iFYVE FENS-1 in the same way as the wild-type protein (Fig. 5). Treatment with wortmannin abolished the localisation of GFP-iFYVE FENS-1 to early endosomes (Fig. 6). Similar results were found in PAE cells (data not shown).

Exogenously expressed DFCP1 is found in the ER and Golgi

The reticular pattern of exogenously expressed Myc-DFCP1 staining co-distributed with a GFP-tagged ER marker protein in fixed COS-7 cells (Fig. 7). The additional perinuclear distribution of Myc or GFP-DFCP1 co-localised strongly with endogenous giantin and gpp130 (Fig. 7 and data not shown), two integral Golgi proteins. However, in cells transfected with Myc-DFCP1, the giantin and gpp130-containing structures were disrupted compared to untransfected cells (Fig. 8 and data not shown). This effect appeared to be in direct proportion to the degree of myc-DFCP1 expression. In low-expressing cells it was possible to see a co-localisation between Myc-DFCP1 and a normal giantin or gpp130 compartment (Fig. 8, arrow), but in brighter cells the Golgi compartment was quite diffuse (Fig. 8). Overexpression of Myc-DFCP1 exerted a similar

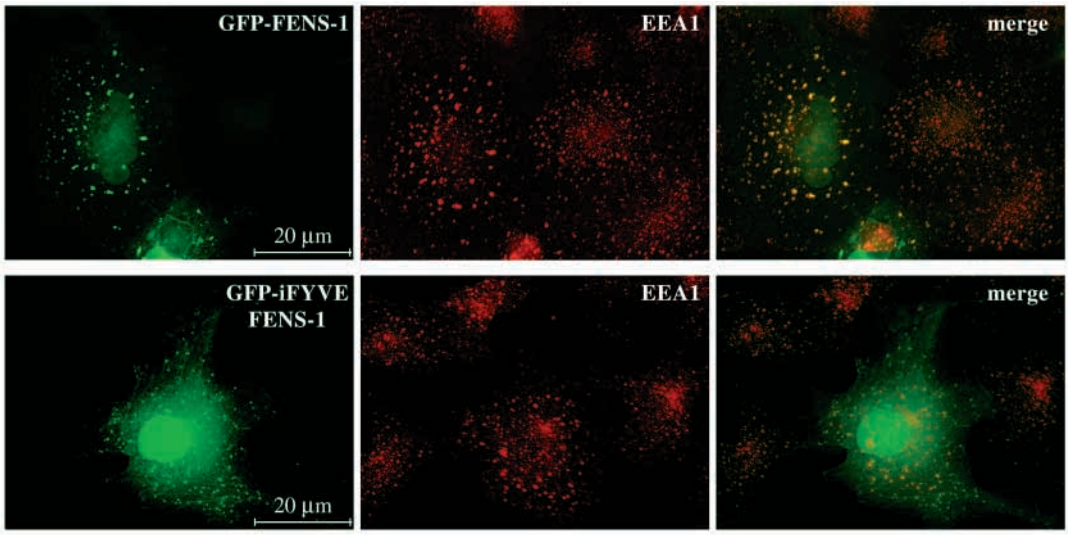

Fig. 5. Colocalisation of GFP-FENS-1 and GFP-iFYVE FENS-1 (the isolated FYVE domain) with the early endosomal marker EEA1. COS-7 cells were transfected with expression vectors encoding GFP-FENS-1 or GFP-iFYVE FENS-1. The cells were fixed with paraformaldehyde and processed for direct (GFP) and indirect immunofluorescence (Texas Red, anti-endogenous EEA1) as described in the Materials and Methods.

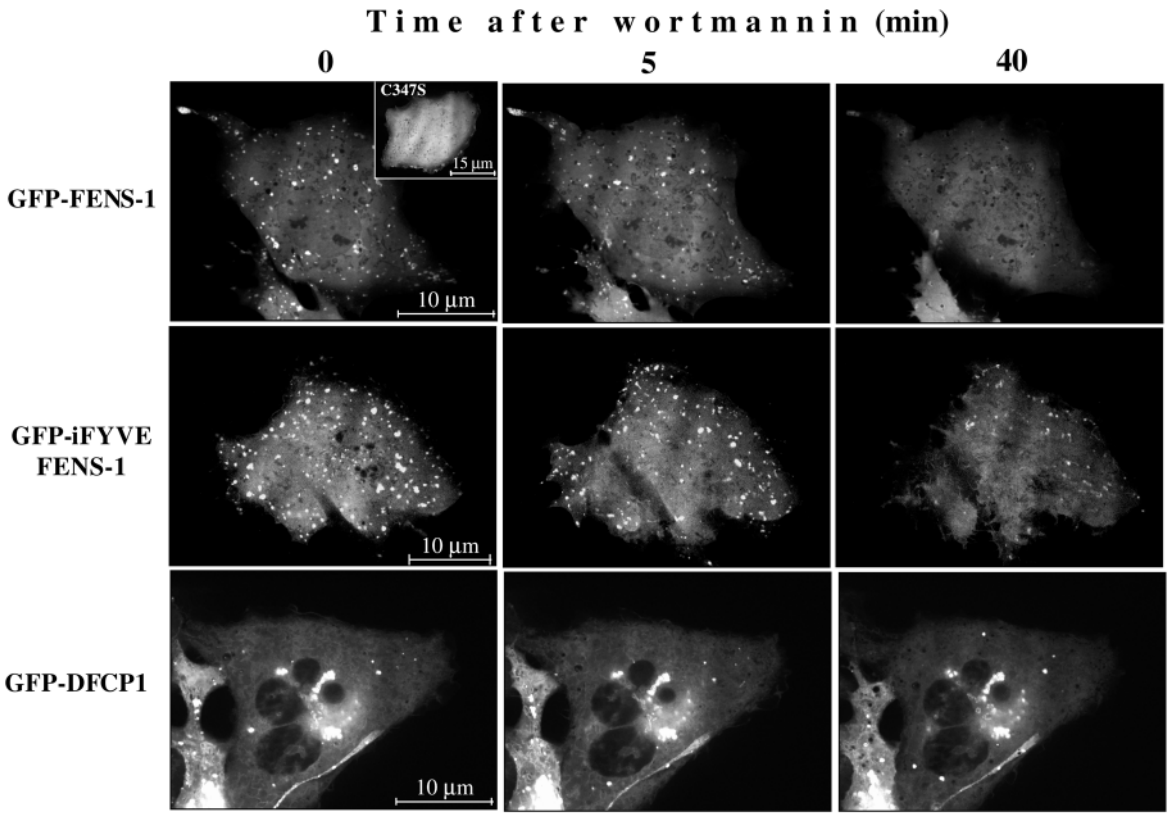

Fig. 6. Effect of wortmannin on the subcellular localisation of GFP-FENS-1, GFP-iFYVE FENS-1 and GFP-DFCP1. COS-7 cells were transfected with expression vectors encoding the indicated GFP-tagged proteins and processed for live image recording of GFP-fluorescence as described in the Materials and Methods. The images shown represent stills taken at the indicated times after 100 nM wortmannin addition: the original videos describing the effects of wortmannin on the localisation of GFP-FENS-1 (Movie A) and GFP-iFYVE FENS-1 (Movie C) can be viewed at jcs.biologists.org/supplemental The cytosolic localisation of GFP-[C347S]FENS-1 is shown as an inset in the top left-hand panel.

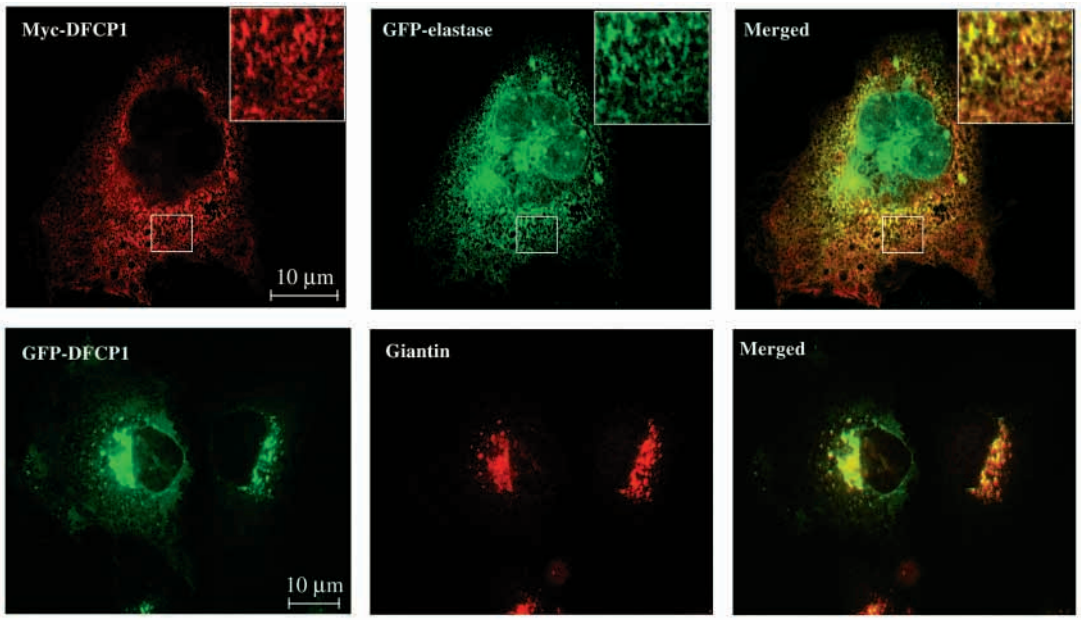

Fig. 7. Colocalisation of exogenously expressed DFCP1 with ER and Golgi markers. Top panels: COS-7 cells were co-transfected with expression vectors encoding GFP-elastase and Myc-DFCP1. Cells were fixed with paraformaldehyde and processed for direct (GFP) or indirect (Texas Red, anti-Myc) fluorescence as described in the Materials and Methods. The images shown were taken at high magnification with a confocal section of <1 μm on a UltraView confocal microscope. Lower panels: COS-7 cells were transfected with an expression vector encoding GFP-DFCP1. Cells were fixed with paraformaldehyde and processed for direct (GFP) or indirect (Texas-Red, anti endogenous giantin) fluorescence as described in the Materials and Methods.

dispersive effect upon the distribution of endogenous β-COP, a component of the COPI coatomer complex, but had no significant effect upon the distribution of endogenous KDEL receptor (data not shown).

The subcellular distribution of exogenously-expressed DFCP1 is governed in part by its FYVE domains but unaffected by wortmannin

The subcellular distribution of the double FYVE-domain mutant of DFCP1, Myc or GFP-tagged [C647S/C770S]DFCP1, was clearly different from that of the wild-type protein (Fig. 8 and data not shown). [C647S/C770S]DFCP1 showed a clear shift to a more condensed, perinuclear distribution that showed strong colocalisation with endogenous Golgi markers (Fig. 8). Furthermore, in contrast to expression of wild-type Myc-DFCP1, expression of Myc-[C647S/C770S]DFCP1 did not cause dispersal of endogenous giantin, gpp130 and β-COP-containing structures but rather appeared to cause their condensation into more compact compartments (Fig. 8 and data not shown).

Brefeldin A (BFA) has been widely used to induce the re-distribution of the Golgi to the ER. The distribution of both wild-type and double-mutant DFCP1 constructs were largely unaffected by treatment with BFA (Fig. 8). However, the integrity of either gpp130- or giantin-containing Golgi structures in cells expressing Myc [C647S/C770S]DFCP1 was substantially resistant to BFA (Fig. 8 and data not shown).

In contrast to FENS-1, a tandem isolated FYVE-domain construct of DFCP1 exhibited a cytosolic distribution in COS-7 cells (Fig. 8, inset), while the subcellular distribution of exogenously expressed Myc or GFP-DFCP1 was unaffected by treatment with wortmannin (Fig. 6 and data not shown).

Exogenously expressed [C647S/C770S] DFCP1 delays arrival of the viral HA protein to the Golgi complex

The electrophoretic mobility of exogenously expressed HA reflects its glycosylation state and is a reliable indicator of its passage through distinct compartments of the early secretory pathway (Lazarovits et al., 1990). HA that is primarily in the ER migrates in SDS gels as a sharp band, whereas HA that has arrived at the Golgi migrates with lower mobility and is more diffuse. Co-expression of HA with FENS-1 had no detectable effect on the transport of HA but co-expression with [C647S/C770S] DFCP1 and to a lesser extent with wild-type DFCP1 had a very significant inhibitory effect on HA-processing (Fig. 9). The extent of inhibition of HA transport with [C647S/C770S] DFCP1 was not as severe as that seen when HA was co-transfected with GTP-bound Arf1 (Arf1(Q71L), Fig. 9), a protein known to block ER to Golgi transport (Kahn et al., 1992), and even at higher levels of expression of the DFCP1 mutant, inhibition of HA transport was not complete (data not shown). However, inhibition of transport was always evident and stronger for the C647S/C770S mutant in comparison with the wild-type protein (Fig. 9 and data not shown). These results extend the morphological results described above indicating the significant effects of DFCP1 and [C647S/C770S] DFCP1 overexpression on Golgi structure and function.

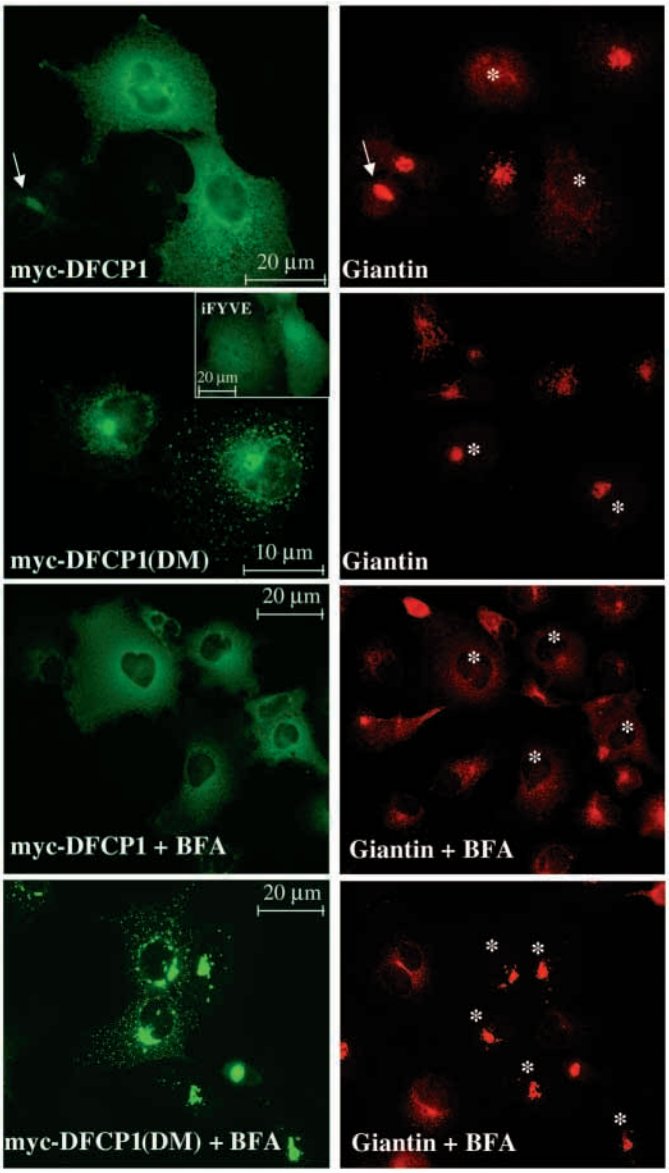

Fig. 8. Effect of exogenous expression of Myc-DFCP1 and Myc-[C647S/C770S]DFCP1 on the morphology of the Golgi. COS-7 cells were transfected with expression vectors encoding Myc-DFCP1, Myc-[C647S/C770S]-DFCP1 (DFCP1(DM)) or the Myc-tagged tandem FYVE-domains of DFCP1 (iFYVE DFCP1; see inset). Where indicated, cells were treated with 2 μg ml^{-1} brefeldin A (BFA) for 20 minutes before fixation. Cells were fixed with paraformaldehyde and processed for indirect immunofluorescence (fluorescein, anti-Myc; Texas-Red, anti endogenous giantin) as described in the Materials and Methods. Cells expressing Myc-DFCP1 or Myc-DFCP1(DM) are marked with an asterisk in the red, giantin images. The arrows mark a cell expressing relatively low levels of Myc-DFCP1 and consequently show good colocalisation of Myc-DFCP1 and an intact, giantin-containing compartment.

DISCUSSION

FENS-1 binds PtdIns3P with clear specificity over other phosphoinositides in the bead displacement assays. Incorporation of low mole % PtdIns3P in PC/PE/PS surfaces can also promote binding of FENS-1 or its isolated FYVE

domain to these surfaces. FENS-1 localises to endosomes in a wortmannin- and FYVE domain-sensitive manner – hence, we suggest the name FENS-1 for FYVE-domain containing protein localised to endosomes. These observations support an emerging model that the FYVE domains in certain proteins bind PtdIns3P and that this interaction plays a role in localising these proteins to PtdIns3P present in early endosomes (Stenmark and Aasland, 1999; Gaullier et al., 1998; Burd and Emr, 1998; Patki et al., 1998). However, the precise roles of PtdIns3P in the endosomal targeting and/or function of most of those proteins is still unclear and initial evidence suggests they may be quite protein specific (Hayakawa and Kitamura, 2000). The best studied example of a PtdIns3P-binding protein is EEA1, where targeting to early endosomes requires both FYVE-domain binding to PtdIns3P and the binding of an adjacent domain to the early endosomal GTPase Rab 5 (Lawe et al., 2000; Simonsen et al., 1998). The different relative sensitivities of the endosomal distributions of EEA1 and FENS-1 to wortmannin, together with the different relative abilities of their isolated FYVE domains to localise to these structures, may imply that the FYVE-domain of FENS-1 has a particularly high affinity for PtdIns3P, sufficient to localise this protein to the endosomes independently of other interactions. The observations that exogenous expression of FENS-1 causes similar swelling and vacuolation of the early endosomal compartment to that seen with expression of its isolated FYVE domain and a tandem FYVE-domain construct of Hrs (Gillooly et al., 2000), suggests this phenomenon is probably caused by a reduction in available PtdIns3P rather than the presence of FENS-1 itself. The primary structure of FENS-1 suggests it will adopt a WD 40 propeller with a protruding FYVE domain, suggesting a logical route forward to identifying its function in this compartment is to search for binding partners.

DFCP1 binds PtdIns3P with similar affinity and specificity (Fig. 3 and data not shown) to FENS-1 in the bead displacement assays strengthening, at least for the N-terminal FYVE domain, the concept that FYVE domains are specific binding modules for this lipid. In contrast to FENS-1, however, DFCP1 had significant affinity for PC/PE/PS or PC, PI or PS-only surfaces and it was difficult to establish the effect of incorporating low mole % PtdIns3P into these surfaces. In addition, in contrast to FENS-1, or to any other FYVE domain-containing protein studied so far, DFCP1 has a distinct ER and Golgi localisation. As with all studies of this type, some concern must remain that this subcellular distribution is based solely on expression of exogenous protein and represents a distortion or exaggeration of the endogenous distribution of DFCP1, particularly in view of the avidity of recombinant DFCP1 for phospholipid surfaces. This issue will probably not be resolved until good antibodies have been raised to endogenous DFCP1 but, we note this subcellular localisation of DFCP1 is unique among some dozen different phosphoinositide-binding proteins being studied in our laboratory.

The insensitivity of the Golgi/ER distribution of DFCP1 to wortmannin, the shift in distribution of the double FYVE-domain mutant of DFCP1 to more condensed Golgi structures, and the cytosolic distribution of the isolated tandem FYVE-domain of DFCP1 all indicate that the predominant Golgi-targeting signal for DFCP1 does not involve binding of its FYVE domains to PtdIns3P. They do not, however, address the question of whether DFCP1 binding of PtdIns3P is physiologically important. It is of course possible that DFCP1 does not bind PtdIns3P in vivo, but the apparently high affinity and specificity of PtdIns3P binding in vitro suggest that it does. The idea that PtdIns3P binding may effect a change in a protein distinct from localisation to the membrane surface where it resides (via allosteric effects of protein-binding partners) is not without precedent. For example, Vac1p is a yeast protein in which FYVE domain binding to PtdIns3P is important for its function in protein sorting from the Golgi to the vacuole, but the localisation of the protein is not dictated by the PtdIns3P binding. Given that there is now a substantial body of evidence that PtdIns3P is concentrated in mammalian cells in early endosomes and the internal membranes of multi-vesicular bodies (Gillooley et al., 2000), this idea would require that the PtdIns3P binding to DFCP1 is in these structures or in a compartment hidden from probes used to measure it so far. In this regard, there is clear evidence that multiple PI3-kinase isoforms exist in the Golgi capable of synthesising PtdIns3P and that some of these are wortmannin insensitive (Hickinson et al., 1997; Jones et al., 1998; Domin et al., 2000). The function of this putative binding of PtdIns3P to DFCP1 is unknown but any explanation that suggests it is involved in passage through/out of the Golgi would explain the Golgi-dispersal and BFA-resistant phenotypes of overexpressed wild-type Myc-DFCP1 and [C647S/C770S]DFCP1 respectively and are consistent with the greater co-localising and dispersal effects on β-COP-containing structures than KDEL receptor-containing structures seen in our studies (KDEL receptor is a component of the early Golgi-ER retrieval mechanism). This explanation is also consistent with the clear inhibitory effect of [C647S/C770S]DFCP1 on HA processing by the Golgi.

While this work was in preparation, a splice variant of DFCP1 was described that corresponds to the 40 kDa C-terminal half of the protein described here and contains the two FYVE-domains (TAFF-1) (Cheung et al., 2001). Recombinant TAFF-1 binds PtdIns3P immobilised on nitrocellulose and GFP-TAFF-1 is localised to Golgi stacks in HeLa cells and HEK-293 cells. These results are in broad agreement with our demonstration that DFCP1 can bind PtdIns3P presented in detergent micelles in vitro, and that heterologously expressed GFP-DFCP1 is concentrated in the Golgi in both PAE cells and COS-7 cells. However, it is interesting that Cheung et al. did not note any

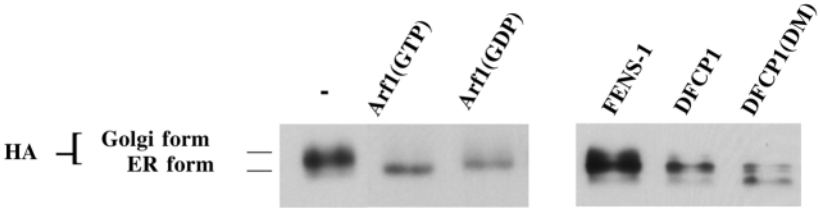

Fig. 9. Exogenous expression of Myc-[C647S/C770S]DFCP1 (DFCP1(DM)) inhibits processing of the HA protein. COS-7 cells were co-transfected with expression vectors encoding HA and one of the indicated proteins. After lysis and immunoprecipitation, the HA was resolved in 10% SDS polyacrylamide gels, blotted and probed with HA-specific antibodies. The ER- and Golgi-forms of HA are indicated.

effect of TAFF-1 expression on Golgi structure or function. Perhaps the 'Golgi-disrupting phenotype' we observed with Myc-DFCP1 is cell type specific, dependent on levels of overexpression (we present some evidence for this, see arrow in Fig. 8) or construct-dependent (we note that the effects are much more pronounced with NT Myc-tagged versus NT GFP-tagged constructs). However, it is also possible that this property resides in the N-terminal half of DFCP1, which contains a further Zn-finger and a nucleotide binding consensus with the potential to confer 'motor properties'. Clearly further work is needed to probe the role of these other conserved domains in DFCP1 before we have a full picture of the determinants of its cellular distribution and its dramatic effects on Golgi structure.

This work was supported by the BBSRC and Isaac Newton Trust. P. T. H. is an Advanced BBSRC Fellow. K. E. A. is a Beit Memorial Fellow and acknowledges support from the Australian National Health and Medical Research Councils, and from the R. G. Menzies Foundation. Z. Y. L. thanks the Cambridge Commonwealth Trust, the ORS scheme, New Hall (Cambridge) and the Tan Kar Kee Foundation (Singapore) for generous financial support. We thank the EPSRC Mass Spectrometry Service (Swansea) for mass spectra.

REFERENCES

Anderson, K. E., Coadwell, J., Stephens, L. R. and Hawkins, P. T. (1998). Translocation of PDK-1 to the plasma membrane is important in allowing PDK-1 to activate protein kinase B. *Curr. Biol.* **8**, 684-691.

Brewer, C. B. (1994). Cytomegalovirus plasmid vectors for permanent lines of polarized epithelial cells. *Methods. Cell Biol*. **43**, 233-246.

Burd, C. G. and Emr, S. D. (1998). Phosphatidylinositol 3-phosphate signalling mediated by specific binding to RING FYVE domains. *Mol. Cell* **2**, 157-162.

Cheung, P. C. F., Trinkle-Mulcahy, L., Cohen, P. and Lucocq, J. M. (2001). Characterization of a novel phosphatidylinositol 3-phosphate-binding protein containing two FYVE fingers in tandem that is tageted to the Golgi. *Biochem. J.* **355**, 113-121.

Cooper, M. A., Try, A. C., Carroll, J., Ellar, D. J. and Williams, D. H. (1998). Surface plasmon resonance analysis at a supported lipid monolayer. *Biophys. Biochim. Acta.* **1373**, 101-111.

Cooper, M. A., Hansson, A., Löfas, S. and Williams, D. H. (2000). A vesicle capture sensor chip for kinetic analysis of binding to membrane-bound receptors. *Anal. Biochem*. **277**, 196-205.

Derubeis, A. R., Young, M. F., Jia, L., Robey, P. G. and Fisher, L. W. (2000). Double FYVE-containing protein 1 (DFCP1): isolation, cloning and characterization of a novel FYVE finger protein from a human bone marrow cDNA library. *Gene* **255**, 195-203.

Domin, J., Gaidarov, I., Smith, M. E. K., Keen, J. H. and Waterfield, M. D. (2000). The Class II phosphoinositide 3-kinase PI3k-$C_2\alpha$ is concentrated in the trans-golgi network and present in clathrin-located vesicles. *J. Biol. Chem.* **275**, 11943-11950.

Gaullier, J. M., Simonsen, A., D'Arrigo, A., Bremnes, B., Aasland, R. and Stenmark, H. (1998). FYVE fingers bind PtdIns3P. *Nature* **394**, 432-433.

Gillooly, D. J., Morrow, I. C., Lindsay, M., Gould, R., Bryant, N. J., Gaullier, J. M., Parton, R. G. and Stenmark, H. (2000). Localization of phosphatidylinositol 3-phosphate in yeast and mammalian cells. *EMBO J.* **19**, 4577-4588.

Hayakawa, A. and Kitamura, N. (2000). Early endosomal localisation of Hrs requires a sequence within the proline- and glutamine-rich region but not the FYVE finger. *J. Biol. Chem.* **275**, 29636-29642.

Hickinson, D. M., Lucocq, J. M., Towler, M. C., Clough, S., James, J., James, S. R., Downes, C. P. and Ponnambelam, S. (1997). Association of a phosphatidylinositol-specific 3-kinase with a human trans-golgi network resident protein. *Curr. Biol.* **7**, 987-990.

Kahn, R. A., Randazzo, P., Serafini, T., Weiss, O., Rulka, C., Clark, J., Amherdt, M., Roller, P., Orci, L. and Rothman, J. E. (1992). The amino terminus of ADP-ribosylation factor (ARF) is a critical determinant of ARF activities and is a potent and specific inhibitor of protein transport. *J. Biol. Chem.* **18**, 13039-13046.

Ktistakis, N. T., Kao, C-Y., Wang, W. and Roth, M. G. (1995). A fluorescent lipid analogue can be used to monitor secretory activity and for isolation of mammalian secretion mutants. *Mol. Biol. Cell* **6**, 135-150.

Jones, S. M., Alb, J. G., Phillips, S. E., Bankaitis, V. and Howell, K. E. (1998). A phosphatidylinositol 3-kinase and phosphatidylinositol transfer protein acts synergistically in formation of constitutive transport vesicles from the trans-golgi network. *J. Biol. Chem.* **273**, 10349-10354.

Lawe, D. C., Patki, V., Heller-Harrison, R., Lambright, D. and Corvera, S. (2000). The FYVE domain of early endosomal antigen 1 is required for both phosphatidylinositol 3-phosphate and Rab 5 binding. *J. Biol. Chem.* **275**, 3699-3705.

Lazarovits, J., Shia, S-P., Ktistakis, N. T., Lee, M-S., Bird, C. and Roth, M. G. (1990). The effects of foreign transmembrane domains on the biosynthesis of the influenza virus hemagglutinin. *J. Biol. Chem.* **265**, 4760-4767.

Lemmon, M. A. and Ferguson, K. M. (2000). Signal-dependent membrane targeting by pleckstrin homology (PH) domains. *Biochem. J.* **350**, 1-18.

Painter, G. F., Grove, S. J. A., Gilbert, I. H., Holmes, A. B., Raithby, P. R., Hill, M. L., Hawkins, P. T. and Stephens, L. R. (1999). General synthesis of 3-phosphorylated myo-inositol phospholipids and derivatives. *J. Chem. Soc. Perkin Trans.* **1**, 923-935.

Painter, G. F., Thuring, J. W., Lim, Z.-Y., Holmes, A. B., Hawkins, P. T. and Stephens, L. R. (2001). Synthesis and biological evaluation of a PtdIns(3,4,5)P_3 affinity matrix. *Chem. Commun*. **2001**, 645-646.

Patki, V., Lawe, D. C., Corvera, S., Virbasius, J. V. and Chawla, A. (1998). A functional PtdIns3P-binding motif. *Nature* **394**, 433-434.

Peterson, M. R., Burd, C. G. and Emr, S. D. (1999). Vac1p coordinates Rab and phosphatidylinositol 3-kinase signaling in Vps45p-dependent vesicle docking/fusion at the endosome. *Curr. Biol.* **9**, 159-162.

Simonsen, A., Lippé, R., Christoforidis, S., Gaullier, J. M., Brech, A., Callaghan, J., Toh, B. H., Murphy, C., Zerial, M. and Stenmark, H. (1998). EEA1 links PI3K function to Rab 5 regulation of endosome fusion. *Nature* **394**, 494-498.

Stenmark, H. and Aasland, R. (1999). FYVE-finger proteins – effectors of an inositol lipid. *J. Cell Sci.* **112**, 4175-4183.

Stephens, L. R., Eguinoa, A., Erdjument-Bromage, H., Lui, M., Cooke, F., Coadwell, J., Smrcka, A. S., Thelen, M., Cadwallader, K., Tempst, P. and Hawkins, P. T. (1997). The G$\beta\gamma$ sensitivity of a PI3K is dependent upon a tightly associated adaptor, p101. *Cell* **89**, 105-114.

Tall, G. G., Hama, H., DeWald, D. B. and Horazdovsky, B. F. (1999). The phosphatidylinositol 3-phosphate binding protein Vac1p interacts with a Rab5 GTPase and a Sec1p homologue to facilitate vesicle-mediated vacuolar protein sorting. *Mol. Biol. Cell*. **10**, 1873-1889.